Magnetic Resonance in Medicine 45:1066–1074 (2001)

VD-AUTO-SMASH Imaging

Robin M. Heidemann, Mark A. Griswold, Axel Haase, and Peter M. Jakob*

Recently a self-calibrating SMASH technique, AUTO-SMASH, was described. This technique is based on PPA with RF coil arrays using auto-calibration signals. In AUTO-SMASH, important coil sensitivity information required for successful SMASH reconstruction is obtained during the actual scan using the correlation between undersampled SMASH signal data and additionally sampled calibration signals with appropriate offsets in *k*-space. However, AUTO-SMASH is susceptible to noise in the acquired data and to imperfect spatial harmonic generation in the underlying coil array. In this work, a new modified type of internal sensitivity calibration, VD-AUTO-SMASH, is proposed. This method uses a VD *k*-space sampling approach and shows the ability to improve the image quality without significantly increasing the total scan time. This new *k*-space adapted calibration approach is based on a *k*-space–dependent density function. In this scheme, fully sampled low-spatial frequency data are acquired up to a given cutoff-spatial frequency. Above this frequency, only sparse SMASH-type sampling is performed. On top of the VD approach, advanced fitting routines, which allow an improved extraction of coil-weighting factors in the presence of noise, are proposed. It is shown in simulations and in vivo cardiac images that the VD approach significantly increases the potential and flexibility of rapid imaging with AUTO-SMASH. Magn Reson Med 45:1066–1074, 2001.

Key words: SMASH; AUTO-SMASH; simultaneous acquisition; PPA; RF coil array; MR image reconstruction

The traditional method for reducing MRI acquisition time has been the use of faster gradient hardware in conjunction with shorter data acquisition periods. Recently developed partially parallel acquisition (PPA) techniques (1–7) allow an elegant and significant reduction in imaging time by using the spatial information inherent in a multiple receiver coil array. In these rapid MRI techniques multiple phase-encoded data are derived in parallel from a single phase-encoded NMR signal.

The simultaneous acquisition of spatial harmonics (SMASH) technique (3) was the first practical PPA method. A factor of two to four savings in scan time has been demonstrated in vivo using SMASH with commercially available radiofrequency (RF) coil arrays, and up to an eightfold increasing in imaging speed has been achieved in phantoms using specialized RF hardware (8). When applied to single-shot imaging, SMASH enables single-shot images with increased spatial resolution without increasing imaging time and without requiring increased gradient performance or increased RF power deposition (9). One notable limitation of the original SMASH imaging technique was its demand on the measurement of component coil sensitivities for spatial harmonic generation. This can be a cumbersome, inaccurate, and time-consuming procedure, which in the worst-case scenario can eliminate the time advantage of the SMASH technique, and thereby limits potential applications of faster imaging with SMASH.

To address these limitations, an internal calibration technique for SMASH imaging, AUTO-SMASH (4), in which coil sensitivity information can be detected during the actual scan by an auto-calibration mechanism, was developed. AUTO-SMASH has the major advantage that the component coil-weights, necessary for SMASH reconstruction, can be determined for each individual scan independently and without a significant increase in imaging time. The advantages of this internal sensitivity reference method are that no extra coil array sensitivity maps have to be acquired, and it provides coil sensitivity information in areas of highly nonuniform spin density.

However, AUTO-SMASH revealed a sensitivity to noise in the experimental data (4), and to residual fold-over artifacts due to mismatch and mixing between the spatial frequency components of the image whenever there are deviations from ideal spatial harmonics. We developed two strategies to overcome these reconstruction imperfections. First, we implemented and analyzed a variable-density (VD)-AUTO-SMASH approach to understand the effect of allocating sampling density and to evaluate its potential for artifact reduction. Second, we reduced coil-weighting fit errors and corresponding image artifacts due to an improved coil-weighting factor estimation. Details of the acquisition, fitting, and reconstruction strategies and their synergetic combination are provided below, along with illustrative results from simulations and imaging experiments. It is shown that the more relaxed requirements in VD-AUTO-SMASH lead to a more reliable reconstruction, with reduced sensitivity to noise in the experimental data and fewer imperfections in the spatial harmonic generation.

THEORY

SMASH/AUTO-SMASH Techniques

To highlight the key features of the VD-AUTO-SMASH approach, we first summarize the basic SMASH/AUTO-SMASH techniques by reviewing some results from Refs. 3 and 4.

In the original SMASH study (3), it was shown that it is possible to reconstruct many lines of *k*-space from a single acquired line. SMASH achieves this encoding efficiency in that it uses combinations of signals from an array of surface coils to directly mimic the spatial-encoding normally performed by phase-encoding gradients. In this approach, signals from the various array components are combined by appropriate linear combinations of component coil signal with different linear weights $n_l^{(m)}$, to generate compos-

Department of Physics, University of Würzburg, Würzburg, Germany.

*Correspondence to: Peter Jakob, Department of Physics, University of Würzburg, Am Hubland, 97074 Würzburg, Germany.
E-mail: peja@physik.uni-wuerzburg.de

Received 15 Septemer 2000; revised 5 December 2000; accepted 21 December 2000.

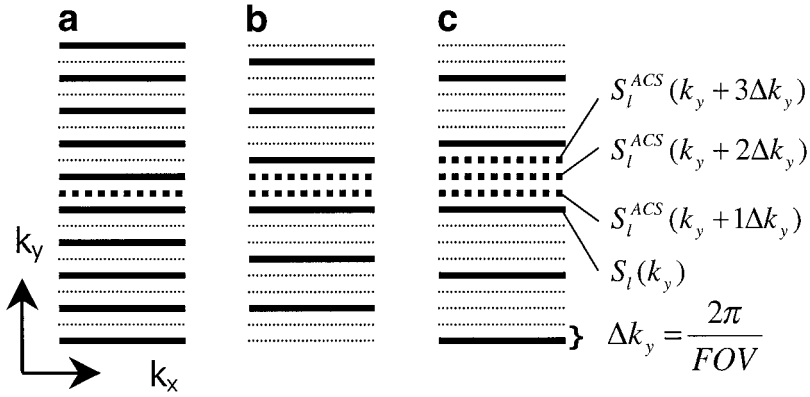

FIG. 1. *k*-Space sampling scheme for AUTO-SMASH. Measured *k*-space lines are indicated by solid lines, missing *k*-space lines are indicated as small-dotted lines, and the additional measured ACS lines at intermediate position are indicated as large-dotted lines. **a:** For a reduction factor $R = 2$, only every second line plus one single ACS line is measured. **b**,**c:** The sampling scheme for reduction factors $R = 3$ and $R = 4$.

ite sensitivity profiles C_m^{Comp} with sinusoidal spatial sensitivity variations (spatial harmonics of order m) on top of the original profile C_0^{Comp}:

$$C_m^{Comp}(x, y) = \sum_{l=1}^{L} n_l^{(m)} C_l(x, y) = C_0^{Comp} \exp\{im\Delta k_y y\}. \quad [1]$$

Here C_l is the coil sensitivity function of coil l at position (x, y), where $l = 1, \ldots, L$ for an L-element array coil, m is an integer that specifies the spatial harmonic number, $i = \sqrt{-1}$, and $\Delta k_y = 2\pi/\text{FOV}$ denotes the minimum k-space interval corresponding to the desired field of view (FOV). If the composite sensitivity profiles generated in this way match the spatial harmonic modulations of phase-encoding gradients, the result is a k-space distribution shifted by precisely the same amount ($m\Delta k_y$) as would have resulted from a traditional gradient step:

$$S_m^{Comp}(k_x,k_y) = \int\int dxdy\, C_m^{Comp}\rho(x,y)\exp\{ik_x x + ik_y y\}$$

$$= \int\int dxdy\, C_0^{Comp}\rho(x,y)\exp\{ik_x x + i(k_y + \Delta k_y)y\}. \quad [2]$$

For accurate reconstruction, the SMASH technique relies upon accurate knowledge or estimation of the relative RF sensitivities of the component coils in the array in order to determine the optimal complex weights $n_l^{(m)}$. Therefore, the most important step in a practical SMASH implementation is to measure the sensitivities of the various array elements. This is a nontrivial problem in vivo, since many factors affect the NMR signal besides coil sensitivity variations, making extraction of coil sensitivity information difficult. There may be additional effects of coil loading that are subject dependent, which can not be easily modeled and may result in unpredictable behavior. In general, in vivo coil sensitivity calibration can be a problematic, inaccurate, time-consuming procedure in many cases—especially in cases with low signal-to-noise ratio (SNR) and tissue motion. This problem occurs in all PPA methods based on the SMASH or the sensitivity encoding (SENSE) (5) approaches.

The AUTO-SMASH approach avoids these limitations by recording a small number of additional autocalibration signals (ACS) during the actual scan. The ACS lines are added to the acquisition, which is shown schematically in Fig. 1 for reduction factors of 2–4 (Fig. 1a–c). In general, if R stands for the reduction factor, $(R-1)$ extra navigator ACS lines are acquired, which are exactly shifted by an amount of $m\Delta k_y$ ($m = 1, \ldots, R-1$). Thus the ACS navigator signals represent lines at intermediate positions in k-space, which are phase encoded in a conventional manner using the phase-encoding gradient. The relation between these navigator reference lines S_l^{ACS} and the usual SMASH signal data lines S_l is then used to "train" SMASH reconstruction directly in k-space. The set of linear weights $n_l^{(m)}$ can be determined automatically, without the intermediate step of coil sensitivity measurements, by using the relations between the conventional SMASH data set and the extra acquired ACS data. A schematic depiction of this procedure is shown in Fig. 2 for a four-element array. The desired optimal complex weights $n_l^{(m)}$, are determined from the following fit function:

$$S^{Comp}(k_y + m\Delta k_y) = \sum_{l=1}^{L} n_l^{(m)} S_l(k_y)$$

$$= \sum_{l=1}^{L} n_l^{(0)} S_l^{ACS}(k_y + m\Delta k_y). \quad [3]$$

In Eq. [3], S^{Comp} stands for the composite ACS, which is shifted precisely $m\Delta k_y$ from the SMASH signal $S_l(k_y)$. This expression can be written in matrix form, which leads to the following equation for a four-element coil array:

$$\underline{S}^{Comp}(k_1, \ldots, k_{Nx}, k_y + m\Delta k_y)$$

$$= (n_1^{(m)} n_2^{(m)} n_3^{(m)} n_4^{(m)}) \begin{pmatrix} \underline{S}_1(k_1, \ldots, k_{Nx}, k_y) \\ \underline{S}_2(k_1, \ldots, k_{Nx}, k_y) \\ \underline{S}_3(k_1, \ldots, k_{Nx}, k_y) \\ \underline{S}_4(k_1, \ldots, k_{Nx}, k_y) \end{pmatrix}. \quad [4]$$

$\underline{S}^{Comp}$ and $\underline{S}_l$ now indicate vectors with N_x elements, where N_x is the number of sampled data points in the read direction. The determination of the unknown coil weights from this overdetermined linear equation system is called an "inverse problem." The solution of this inverse problem can be obtained, for example, with the "pseudoinverse":

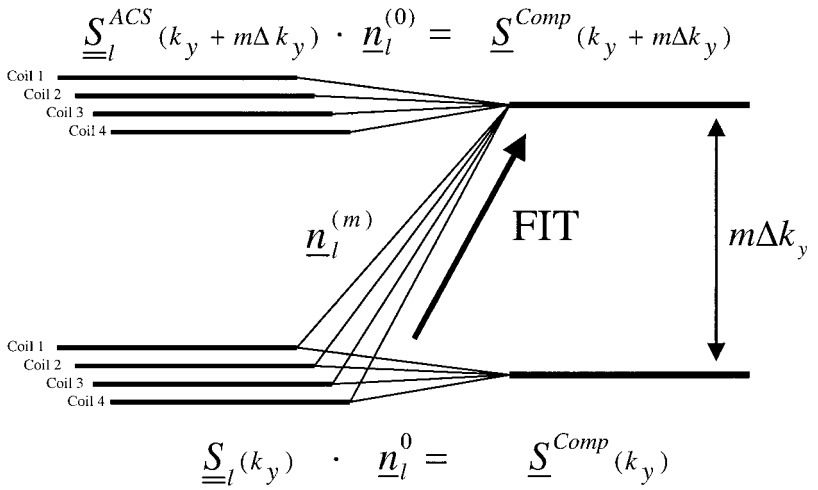

FIG. 2. Determination of the coil weights for a four-element array coil. Here, measured SMASH lines $S_l(ky)$ are fitted to a single composite ACS line $S^{Comp}(ky+m\Delta ky)$, which is shifted by $m\Delta ky$, yielding the desired coil weights.

$$\underline{n}_l^{(m)} = \underline{S}^{Comp}\underline{S}_l^*(\underline{S}_l\underline{S}_l^*)^{-1}. \quad [5]$$

In Eq. [5], $\underline{n}_l^{(m)}$ stands for the vector of the l complex coil-weights, $\underline{S}^{Comp}$ is the vector of the composite ACS, and $\underline{S}_l^*$ is the transposed complex conjugate matrix of the l-SMASH data lines. Implementation of the problem in this way also facilitates the incorporation of numerical conditioning into the process. The pseudoinverse that was implemented for this work included numerical conditioning using a singular value decomposition, followed by a singular value threshold.

In summary, the AUTO-SMASH self-calibration procedure replaces an experimentally cumbersome and potentially inaccurate coil sensitivity measurement with a targeted acquisition of a few extra lines of NMR signal data. Acquisition of the extra $(R-1)$ navigator lines adds only a very small amount to the total acquisition time, and allows direct "sensitivity calibration" for each image, even in regions of inhomogeneous spin density and regardless of coil loading. If flexible coil arrays are used, AUTO-SMASH can provide accurate calibrations even if array positions change from scan to scan.

However, both AUTO-SMASH and SMASH presume that the coil-encoding procedure provided by the underlying array matches the conditions of Fourier encoding precisely. Thus, these PPA techniques presume that the necessary spatial harmonics may be faithfully represented by linear superposition of component coil sensitivities. In situations where the combined sensitivities deviate from ideal spatial harmonics, reconstruction artifacts occur as residual fold-over artifacts in both AUTO-SMASH and SMASH reconstruction. Thus, AUTO-SMASH and SMASH share the same operating limits in that they require the sensitivity functions of individual coils in an array to generate spatial harmonics for a given FOV and slice position. In addition, the coil sensitivity fitting procedure in SMASH and the self-calibration approach in AUTO-SMASH are both affected by noise in the experimental data, resulting in significant reconstruction artifacts in the low-SNR regime (4).

VD-AUTO-SMASH: Principles

The concept of improving the image quality by using a variable-density approach is based on the assumption that some parts of k-space can be measured with more accuracy than others. In most imaging situations, the importance of k-space lines decreases with increasing phase-encoding values. This is the essential basis for many imaging concepts and also the essential basis for the VD-AUTO-SMASH approach. VD-AUTO-SMASH is, in spirit, similar to the work presented by Luk et al. (11), who addressed flow artifacts in echo-planar imaging; Weiger et al. (12), who examined respiratory motion artifacts; and Tsai and Nishimura (13), who addressed aliasing artifacts using a VD k-space sampling trajectory. Since AUTO-SMASH is a k-space related PPA technique, it is well suited to VD sampling. In this approach we reduce residual aliasing artifacts by exploiting the fact that in most images the energy is concentrated around the k-space origin.

If k-space is uniformly undersampled, then aliasing artifacts will be dominated by low-frequency components. These low-frequency, high-energy artifacts can be avoided in imperfect AUTO-SMASH reconstruction by sampling the central k-space with a density corresponding to a standard full FOV acquisition. The sampling density above a certain cutoff-spatial frequency (COSF) is then decreased to a "standard" SMASH density, $1/R$. In the outer parts of k-space above the COSF the reduction factor is R, which we now refer to as the outer reduction factor (ORF). The new k-space sampling pattern for VD-AUTO-SMASH is shown schematically in Fig. 3c. For comparison, the k-space sampling scheme of a full time reference acquisition (Fig. 3a) and the conventional AUTO-SMASH acquisition (Fig. 3b) are shown. In the same figure the corresponding sampling density functions are plotted on the bottom row.

Thus, in VD-AUTO-SMASH several ACS lines for each harmonic are acquired in the center of k-space. In the following, it is demonstrated that these extra acquired lines reduce high-energy fold-over artifacts when they are included in the final image reconstruction, while at the same time they also allow an improved determination of the coil weights. In general, the improvement with this VD approach comes at the expense of a longer minimum scan time, which adds $(R-1+N^{extra})\times T$ to the SMASH scan time, where N^{extra} stands for the number of additional acquired ACS lines in the center of k-space, and T represents the repetition time or interecho spacing of the applied imaging technique.

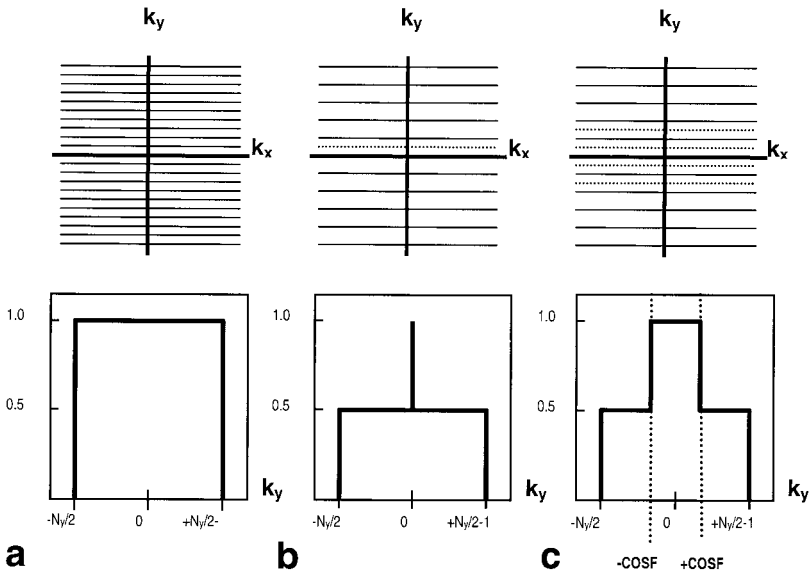

FIG. 3. *k*-Space sampling scheme for (**a**) the reference scan, (**b**) an AUTO-SMASH acquisition with reduction factor of 2 (one ACS line), and (**c**) the VD-AUTO-SMASH approach with three additional ACS lines. On the bottom row, the corresponding density functions are plotted schematically.

Improved Coil-Weighting Factor Estimation: Principles

In general, image quality in reconstructed SMASH/AUTO-SMASH images depends on how well the coil-weighting factors can be extracted from the experimental data. Thus the issue of contaminating noise in the data has to be addressed, since any large error in the fit procedure results in residual aliasing in the reconstructed image (see, e.g., Ref. 4). One important practical aspect of the VD-AUTO-SMASH acquisition is the possibility of improved fitting, achieving a reduction in the variability of the coil-weighting factor estimation. In the following we present an algorithm that allows one to extract improved values of the coil-weighting factors from noise-corrupted ACS observations. In the original AUTO-SMASH approach, only one fit between two single lines was used to determine the coil weights for the corresponding shift in *k*-space. In the VD approach, the acquisition of extra ACS lines provides the possibility of improving this fit by taking advantage of the several additional fitting combinations. This is shown schematically in Fig. 4 for VD-AUTO-SMASH acquisitions with ORF = 4, and six ACS lines in total. In the original AUTO-SMASH approach, just one fitting combination would be used to determine the first coil weights (see Fig. 4a). The more sophisticated VD-AUTO-SMASH scheme shown in Fig. 4b enables seven additional fits (eight total).

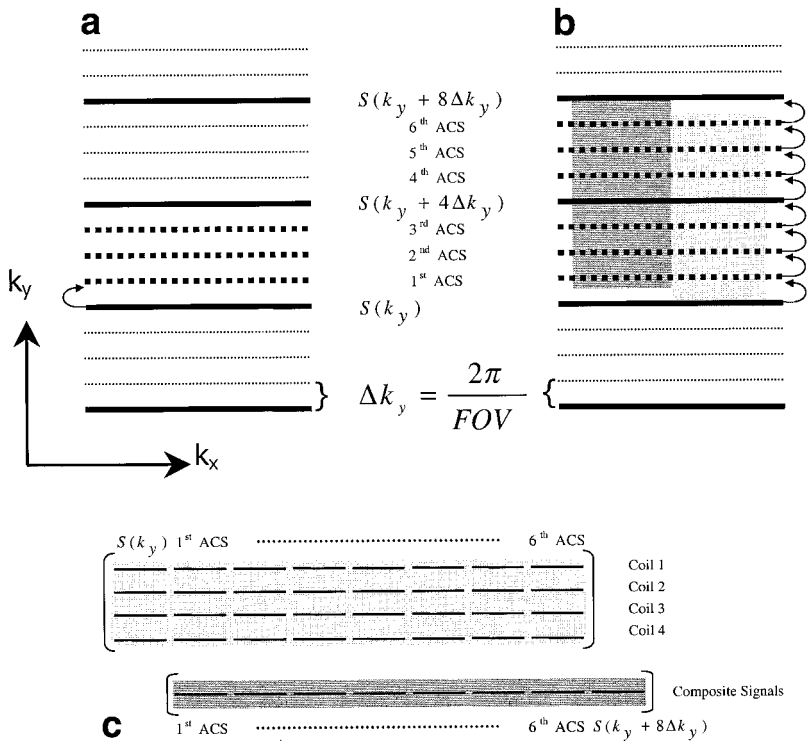

FIG. 4. AUTO-SMASH/VD-AUTO-SMASH acquisition schemes. **a:** In AUTO-SMASH only the fit between the SMASH line and the corresponding ACS line is used to determine the coil weights. **b:** The improved scheme of the VD approach enables seven additional fits. **c:** Graphical depiction of how to combine the signals to generate the enlarged matrix of the coil data sets (bright gray block) and the enlarged vector of the composite signals (dark gray block).

One straightforward approach would be to simply average these eight sets of fitted coil weights. The main drawback of this approach is that the estimation of coil weights with ACS lines from the outer part of *k*-space, with significantly reduced SNR, is strongly affected by noise (see Ref. 4). The *weighted averaging* scheme (Fig. 4b) used in this work takes the signal energy content of each particular *k*-space line into account. The two regularly measured SMASH lines $S_l(k_y + m\Delta k_y)$ (with $m = 0$,) and the six ACS lines $S_l(k_y + m\Delta k_y)$ (with $m = 1,2,3,5,6,7$) are composed in such a way that these eight coil data sets built an $8 \cdot N_x \times N_{Coil}$ coil data matrix, where N_x is the number of sampled points in the read direction and N_{Coil} is the number of coils in the array. This is shown schematically in Fig. 4c, where the data sets of the above-described lines, which are indicated by the bright gray block, are stacked into a matrix. The vector of the composite signals is constructed in the same manner, but every line is shifted by Δk_y (indicated by the dark gray block in Fig. 4c). The estimation of the coil weights is then performed with a fit between the enlarged matrix and the enlarged vector. In this example, the matrix and vector are eight times larger than those in Fig. 2. In Fig. 4 only the estimation of the coil weights, $n_l^{(1)}$, for a shift about Δk_y is indicated. However, it is straightforward to apply the same procedure for larger shifts in *k*-space. By computing the pseudoinverse in this way, the relative contribution of the different lines is weighted by the square of their intensity, which is equivalent to the energy of the respective *k*-space lines.

METHODS

Simulated VD-AUTO-SMASH Imaging

The possible benefit of VD sampling was first explored with computer simulations in order to have a well-controlled imaging situation. First, simulated coil maps were generated using an analytic integration of the Biot-Savart equation, which was implemented in the Matlab programming language (The Mathworks, Natick, MA). The geometry of the underlying array, described below, is exactly the same as for the in vivo experiments. For these simulations, an image plane parallel to the plane of the linear coil array, approximately 10 cm from the coil's surface, was assumed. Once simulated coil field maps were generated, simulated VD-AUTO-SMASH imaging was performed in the IDL programming environment (Research System Inc., Boulder, CO), using an image of the well-known Shepp-Logan phantom. Simulated raw data sets with a matrix size of 144×256 were generated with noise levels corresponding to typical in vivo applications. The VD-AUTO-SMASH images were reconstructed with various ORFs from 2 to 4 and a variable number of ACS lines in the center of *k*-space.

In Vivo VD-AUTO-SMASH Imaging

For initial demonstration of the VD approach, VD-AUTO-SMASH was also applied to routine cardiac scans that were generated on a Siemens Vision 1.5 Tesla whole-body clinical MR scanner (Siemens Medical Systems, Erlangen, Germany). All raw data were obtained with a standard gradient coil (rise time of 600 μs to a peak gradient amplitude of 25 mT/m along all three axes) and the prototype cardiac coil array described in Ref. 10. This array coil consists of four overlapped component coils, with a total spatial extent of 260 mm in the phase-encoding direction and 230 mm in the read direction. The array extends in the head–foot direction, and was used in a receive-only mode, with the body coil providing homogeneous excitation. During transmit, the array was actively decoupled from the body coil. For imaging, a segmented turbo-FLASH with nine lines per segment was used: flow compensation in the slice and read directions, and an incremented flip angle series (18°, 20°, 22°, 25°, 31°, 33°, 38°, 48°, and 90°). A TR of 14.4 ms and TE of 7.3 ms resulted in an effective temporal resolution of 131 ms. The images were obtained during a single end-expiratory breathhold with the subjects in a prone position above the coil array. The image matrix was 144×256 for all reference scans. Healthy volunteers were examined according to the guidelines of the internal review board of the Beth Israel Deaconess Medical Center. Informed consent was obtained before each study[1]. Fitting of the coil-weighting functions and image reconstruction were performed in the IDL programming environment (Research System Inc., Boulder, CO). To investigate the potential of the VD approach, data sets with a varying number of ACS lines and ORFs from 2 to 4 were generated retrospectively by removing the appropriate number of *k*-space lines from the full time reference data set.

Artifact Power

The resulting images, at each of the different acceleration factors for the simulations and the in vivo data, were subjected to a quantitative evaluation of the total artifact power *P*. *P* is defined as the overall power of an artifact image I_a, which is obtained by the complex difference of a VD-AUTO-SMASH image I_{VD} and a hypothetical, i.e., artifact-free, image I. In detail, the total artifact power *P* is the total power in the complex difference image, found by subtracting the reference and the VD-AUTO-SMASH images and squaring the magnitude of the result, divided by the total power in the reference image, found by squaring the magnitude of the reference image. In this manner, artifact power was evaluated using a full FOV reference and various VD-AUTO-SMASH reconstructions. The reference image without any acceleration was generated using a simple phased-sum reconstruction as in Refs. 3, 4, 8, and 14. The reader should keep in mind that the artifact power could be artificially elevated due to noise, even when the folding artifacts are completely removed.

The artifact power vs. the total number of acquired *k*-space lines, which corresponds to the scan time, was plotted to evaluate the dependence between artifact power and acquisition time for different reconstruction methods. The curves for the different ORFs always start with the minimum amount of ACS lines for an AUTO-SMASH reconstruction (see Fig. 1). The stepwise acquisition of additional ACS lines was done in a centric reordered manner.

[1]It should be noted that the raw scans used in this study were first used in a recent study of cardiac imaging with AUTO-SMASH (4).

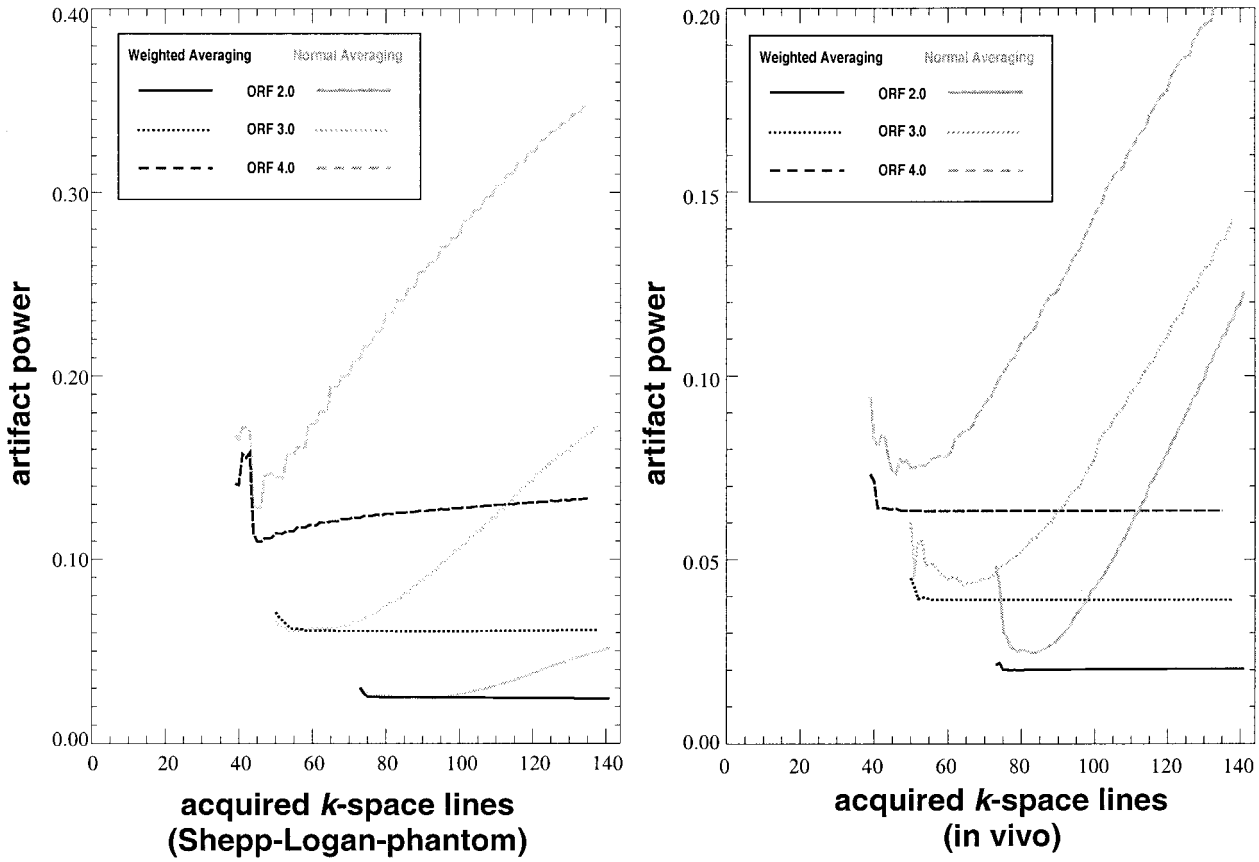

FIG. 5. Artifact power vs. the total number of acquired lines. Left graph: VD-AUTO-SMASH acquisition with noise for the Shepp-Logan phantom. Right graph: VD-AUTO-SMASH acquisition for the in vivo data. To investigate the influence of the fit, the ACS lines were used only to improve the determination of the coil weights. For comparison, the results achieved with normal averaging (gray curves) and weighted averaging (black curves) are plotted in the same graph.

This means that the distance of the ACS lines from the *k*-space center was increased with the increasing number of additional lines.

RESULTS

To demonstrate the effects of the VD approach in combination with the improved coil-weight fitting procedure, a number of phantom and cardiac data sets are presented.

We first show that the operation of stacking and fitting multiple ACSs in parallel leads to an increased accuracy beyond that provided by a single ACS line. In Fig. 5 the calculated artifact power vs. the total number of acquired *k*-space lines is plotted. In Fig. 5 the results obtained (left column) for simulations using the Shepp-Logan phantom with an SNR of 40, and (right column) for simulations using the in vivo data are shown. To investigate the influence of the fit, all acquired ACS lines were used only to improve the fit by averaging the estimated sets of coil weights. This means that the ACS lines were not used to replace reconstructed lines in *k*-space, so the number of measured and reconstructed lines in *k*-space used for image generation stays constant. For the normal averaging method (gray curves), there is first a rapid decrease in artifact power within only a few extra ACS lines. However, further acquisition of ACS lines leads to an increasing artifact power, since the outer lines contribute more noise than signal. In contrast, the weighted averaging method (black curves) achieves a constant artifact power level after a few ACS lines. Especially in case of the in vivo data, the use of the weighted averaging method has two effects on the artifact power curve. First, the minimum artifact power level is significantly lower than that for the conventional averaging. Second, the fall off the fit with increasing distance of the ACS lines is completely prevented. The most important aspect of these simulations is that just a few additional ACS lines are necessary to reach the minimum level of artifact power.

To demonstrate the efficiency of the VD method in image space, simulations for the Shepp-Logan phantom with an SNR of 40 and an image size of 144×256 are shown in Fig. 6. The conventional AUTO-SMASH reconstruction, with a reduction factor $R = 2$ and the minimum amount of one ACS line (Fig. 6b), is suboptimal at this level of acceleration. The calculated acceleration factor is 1.97 in this case, since data acquisition was performed in 51% of the total reference scan time. Using an acceleration factor of 2.0, VD-AUTO-SMASH with ORF = 4, and 33 additional ACS lines, leads to the image in Fig. 6c. Compared to the reference image (Fig. 6a) this VD-AUTO-SMASH image shows essentially equivalent image quality. To highlight

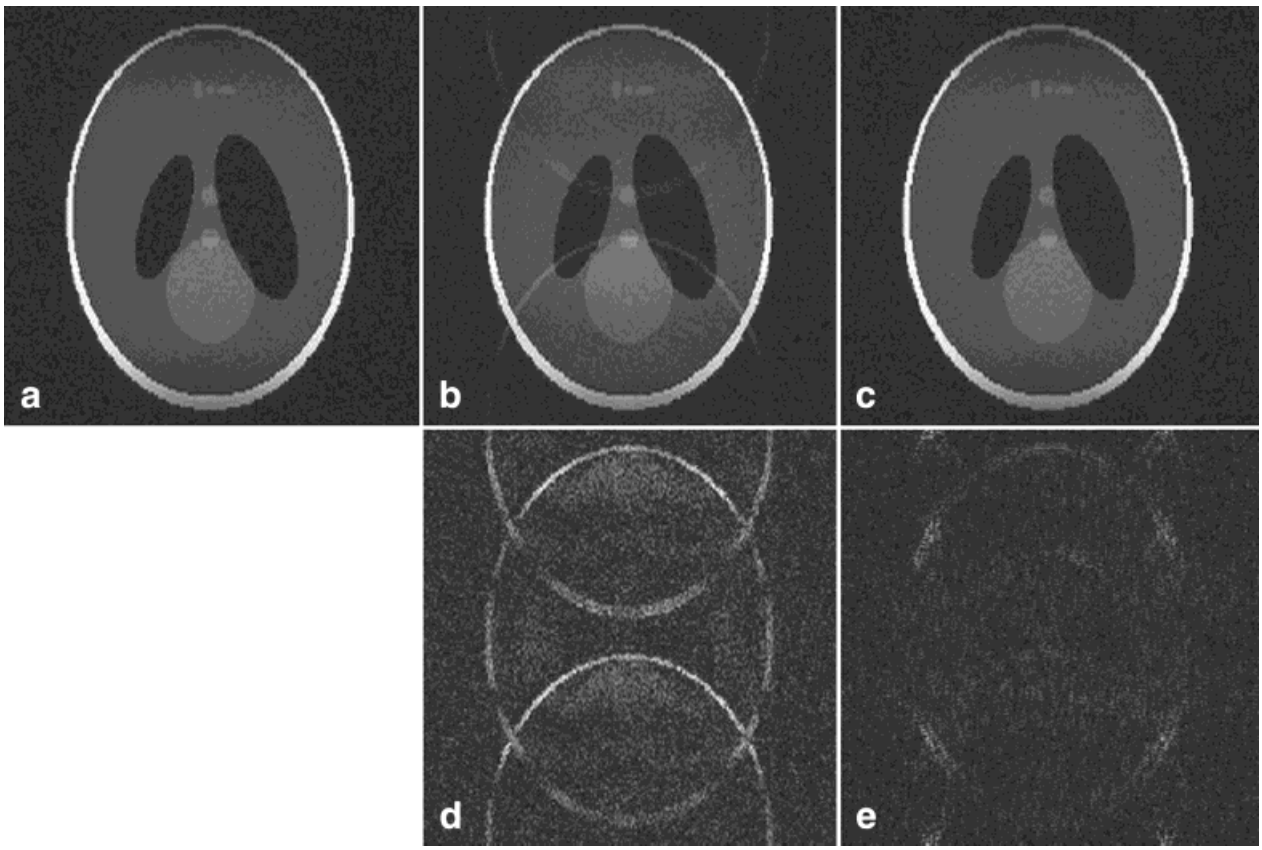

FIG. 6. Imaging results for the Shepp-Logan phantom simulations using a four-element array coil for two different acquisition schemes. **a:** The reference image with a matrix size of 144 × 256, and 100% acquisition time. **b:** The conventional AUTO-SMASH image. A single set of coil weights was used for the reconstruction; the acceleration factor is 1.97 (51% of the scan time). **c:** In the same scan time, a VD-AUTO-SMASH image with 33 additional ACS lines is acquired; the acceleration factor is 2.0 (50% of the scan time). Bottom row: The corresponding difference images (scaled to highlight the artifacts) (**d**) between the conventional AUTO-SMASH image and the reference, and (**e**) between the VD-AUTO-SMASH image and the reference.

the remaining image artifacts, corresponding difference images between the reference and the reconstructed images are shown in the bottom row.

The combination of improved coil-weighting factor estimation and full sampling density in the center of *k*-space leads to the artifact power curve shown in Fig. 7 for the in vivo data. Here the extra acquired data sets are used to improve the fit and to replace reconstructed lines in the center of *k*-space with the phased sum of these ACS lines. This graph summarizes two major results. First, it is clearly visible that the same artifact power level could be achieved faster with the ORF = 4 acquisition than with the ORF = 2 acquisition (indicated by the horizontal line between position a-b in Fig. 7). This can be explained by the increased area with full FOV sampling in the center of *k*-space, where most of the *k*-space energy is located. Second, at an acceleration factor of 2.0 (indicated by the vertical line between position a-c in Fig. 7), the best result (the least artifact power) is achieved with ORF = 4. It should be stressed that the obtained results were achieved with data sets that were generated retrospectively from full time reference data. Thus, additional benefits such as reduced motion artifacts could be expected from actual accelerated acquisitions.

As demonstrated by these results, VD-AUTO-SMASH allows a flexible trade-off between image quality and acquisition time. To demonstrate the benefits and efficiency of the combined VD approach in image space, a set of representative in vivo images (image matrix 144 × 256) is shown in Fig. 8, demonstrating the efficiency of the proposed VD approach. The most remarkable aspect of VD-AUTO-SMASH image is the lack of any large artifacts, as demonstrated by the difference image in the bottom row (see Fig. 8e). This image was obtained in just 50% of the reference image scan time.

DISCUSSION

In general, PPA techniques are used to reduce scan time beyond the limits of purely gradient-encoded imaging experiments. However, at the same time it is necessary to find an acceptable compromise between the desired scan time reduction and the image quality obtained. Thus, the PPA speed advantage should be optimized in such a way as to obtain the best possible result. To achieve this goal, we used the importance of the center of *k*-space to motivate the sampling density in VD-AUTO-SMASH imaging. In the present work, two types of improvement due to VD sampling were investigated: 1) the reduction of image artifacts effects due to a more full coverage of important low-spatial frequency data, and 2) the improved determi-

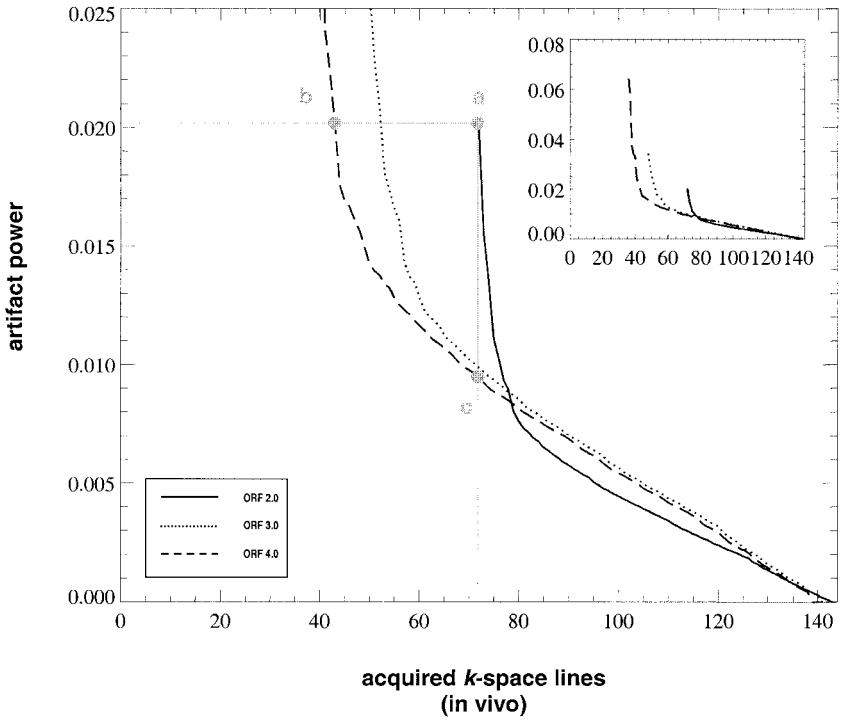

FIG. 7. Artifact power vs. the total number of acquired lines for in vivo VD-AUTO-SMASH acquisition. The additional acquired ACS lines are used to improve the fit and to replace the reconstructed lines in the center of *k*-space. Further details are described in the text.

nation of coil-weighting factors. The simulations and experiments performed in this work clearly demonstrate the capability of VD-AUTO-SMASH to obtain images with significantly increased image quality compared to standard SMASH/AUTO-SMASH reconstruction. In this study, we have demonstrated reductions of scan time by 30–70% with respect to pure Fourier encoding for in vivo imaging using a four-element coil array. A reduction in scan time of approximately 30–70% corresponds to the range between positions c and a in the graph shown in Fig. 7. In addition, it was clearly demonstrated that comparable artifact levels can be achieved faster with high ORF acquisitions, since in this case more acquisition time is available to sample the low-spatial, high-energy *k*-space data. On the other hand, VD-AUTO-SMASH can achieve reduced artifact levels in the same image acquisition time using high ORFs.

The most important key parameter for VD-AUTO-SMASH optimization is the choice of the optimal COSF. The COSF is difficult to quantify in general. The optimal COSF is a complex function of many variables, including the spin density of the object to be imaged and the performance of the array. This also depends on the choice of the imaging plane, the desired image quality, and the imaging application. In general, the COSF should be large enough to provide sufficient fold-over suppression but no larger than necessary to preserve the speed benefits of PPA imaging. However, it should be stressed that in most imaging situations, some level of image quality reduction is guaranteed compared to the full time acquisition, since there is still important information in the periphery of *k*-space.

We are currently investigating optimum sampling densities for various applications, since the spatial frequency content for different applications may be quite distinct. Therefore, it is clear that the density distribution should be matched to the desired application. Further evaluation and optimization of the *k*-space density distribution is required. However, some initial insight concerning $COSF_{Opt}$ can be gained from the plot of the integrated *k*-space energy vs. the *k*-space position. This kind of graph can lead to a first guess concerning *k*-space energy and related artifact power distributions. However, the first step in the process would be for the user to decide on an acceptable imaging quality for a given application and acceleration factor. In cases in which optimal image quality is needed, the corresponding VD-AUTO-SMASH will most likely demand a high COSF factor. In applications in which a rapid acquisition is the primary goal, a higher level of artifact may be tolerated, and therefore a low COSF factor can be used. In addition, there are many possible choices of sampling densities that can be tailored to the specific application of interest. For cases in which the most *k*-space energy is expected in the low-spatial-frequency components, a sampling density such as the one shown in Fig. 3c could be used. On the other hand, for applications such as cardiac tagging or angiography, a more homogeneous sampling density might be optimal, since small objects contain equal energy at all spatial frequencies. In general, arbitrary sampling densities can be designed. Finally, a subtle yet important result of this work is that the VD-AUTO-SMASH approach works at arbitrary reduction factors between 1 and the number of coils used.

CONCLUSIONS

In the present work a new, improved approach for the AUTO-SMASH imaging method using a VD acquisition in combination with self-calibration signals was introduced and examined. The features were compared with conventional AUTO-SMASH and standard imaging experiments

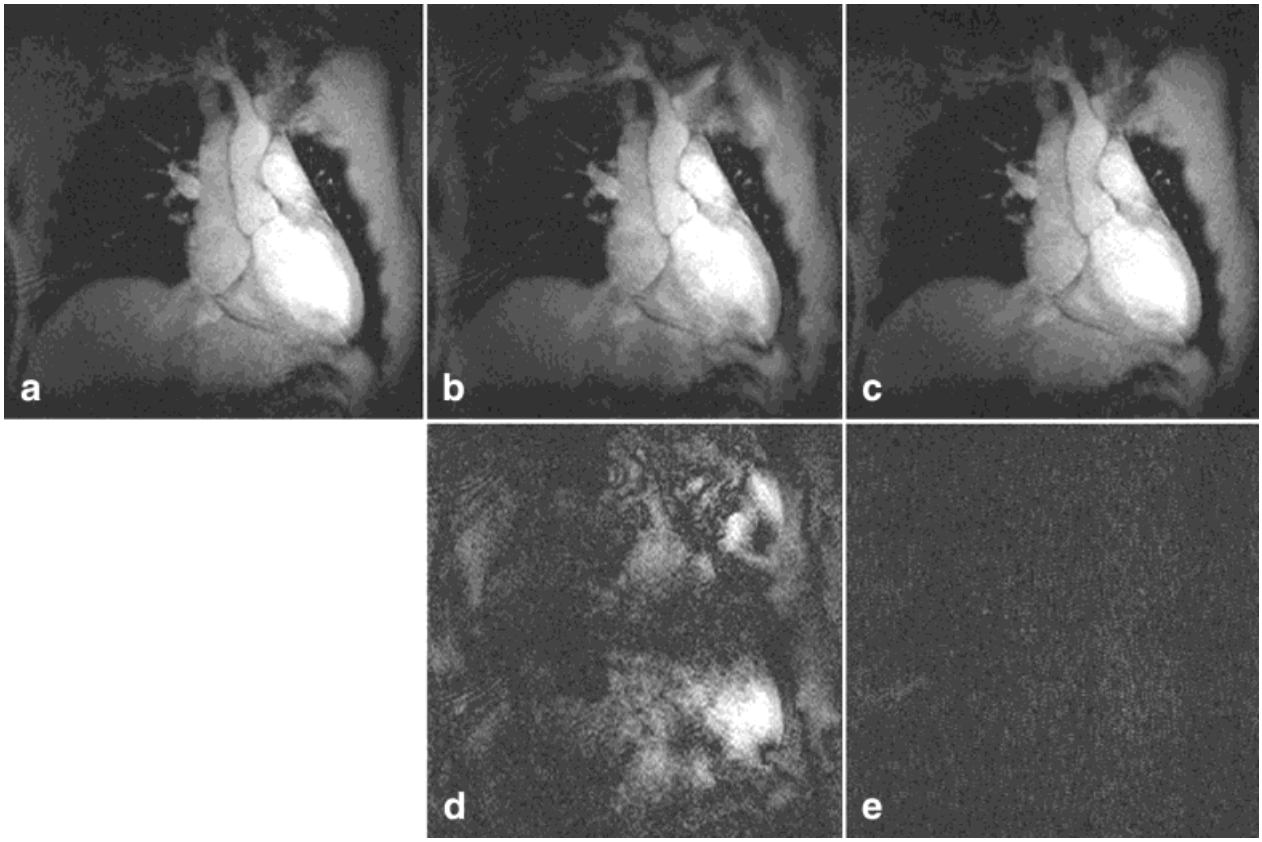

FIG. 8. Cardiac imaging with VD-AUTO-SMASH using a four-element array coil for different acquisition schemes. **a:** The reference image obtained in 16 cardiac cycles with 144 × 256 matrix size, and 100% acquisition time. **b:** The conventional AUTO-SMASH image. A single set of coil weights was used for the reconstruction; acceleration factor is 1.97 (51% of the scan time). **c:** A VD-AUTO-SMASH image with ORF = 4 and 33 additional ACS lines; the acceleration factor is 2.0 (50% of the scan time). This result was obtained in the same time as the conventional AUTO-SMASH image. Bottom row: The corresponding difference images (scaled to highlight the artifacts) (**d**) between the conventional AUTO-SMASH image and the reference, and (**e**) between the VD-AUTO-SMASH image and the reference.

in simulations based on simulated and in vivo data. The possible advantages are a significantly increased image quality in moderately increased imaging times. The VD-AUTO-SMASH approach allows one to find a good compromise between scan time and image quality, which can be adjusted freely to the imaging requirements. However, one essential prerequisite for VD-AUTO-SMASH is the capability of the underlying array to provide combined sensitivities that match the conditions of Fourier encoding. Finally, the use of additionally sampled calibration signals, as demonstrated with VD-AUTO-SMASH, may play an important role in other parallel imaging techniques, such as partially parallel imaging with localized sensitivities (PILS) (6).

ACKNOWLEDGMENTS

The authors thank D.K. Sodickson for helpful discussions.

REFERENCES

1. Carlson JW, Minemura T. Imaging time reduction through multiple receiver coil data acquisition and imaging reconstruction. Magn Reson Med 1993;29:681–688.
2. Ra JB, Rim CY. Fast imaging using subencoding data sets from multiple detectors. Magn Reson Med 1993;30:142–145.
3. Sodickson DK, Manning WJ. Simultaneous acquisition of spatial harmonics (SMASH): fast imaging with radiofrequency coil arrays. Magn Reson Med 1997;38:591–603.
4. Jakob PM, Griswold MA, Edelman RR, Sodickson DK. AUTO-SMASH: a self-calibrating technique for SMASH imaging. MAGMA 1998;7:42–54.
5. Pruessmann KP, Weiger M, Scheidegger B, Boesiger P. SENSE: sensitivity encoding for fast MRI. Magn Reson Med 1999;42:952–962.
6. Griswold MA, Jakob PM, Nittka M, Goldfarb JW, Haase A. Partially parallel imaging with localized sensitivities (PILS). Magn Reson Med 2000;44:602–609.
7. Kyriakos WE, Panych LP, Kacher DF, Westin CF, Bao SM, Mulkern RV, Jolesz FA. Sensitivity profiles from an array of coils for encoding and reconstruction in parallel (SPACE RIP). Magn Reson Med 2000;44:301–308.
8. Bankson JA, Griswold MA, Wright SM, Sodickson DK. SMASH imaging with an eight element multiplexed RF coil array. MAGMA 2000;10:93–104.
9. Griswold MA, Jakob PM, Chen Q, Goldfarb JW, Manning WJ, Edelman RR, Sodickson DK. Resolution enhancement in single-shot imaging using simultaneous acquisition of spatial harmonics (SMASH). Magn Reson Med 1999;41:1236–1245.
10. Griswold MA, Jakob PM, Edelman RR, Sodickson DK. A multicoil array designed for cardiac SMASH imaging. MAGMA 2000;10:105–113.
11. Luk Pat GT, Meyer CH, Pauly JM, Nishimura DG. Reducing flow artifacts in echo-planar imaging. Magn Reson Med 1997;37:436–447.
12. Weiger M, Börnert P, Proksa R, Schäfter T, Haase A. Motion-adapted gating based on k-space weighting for reduction of respiratory motion artifacts. Magn Reson Med 1997;38:322–333.
13. Tsai C-M, Nishimura DG. Reduced aliasing artifacts using variable-density k-space sampling trajectories. Magn Reson Med 2000;43:452–458.
14. Sodickson DK. Tailored SMASH image reconstructions for robust in vivo parallel MR imaging. Magn Reson Med 2000;44:243–251.